**Pergamon**

0731–7085(94)E0002-I

# A spectroscopic investigation of DuP 747 polymorphs

KRISHNASWAMY RAGHAVAN,*† ANIL DWIVEDI,† G. CRESTON CAMPBELL JR,‡ GREGORY NEMETH† and MUNIR A. HUSSAIN†

† *The DuPont Merck Pharmaceutical Co., Experimental Station, P.O. Box 80400, Wilmington, DE 19880-0400, USA*
‡ *The DuPont Co., Experimental Station, P.O. Box 80328, Wilmington, DE 19880-0328, USA*

**Abstract:** DuP 747, a selective kappa agonist analgesic, was found to have at least two polymorphic forms, and this was confirmed by X-ray powder diffraction. DSC and thermomicroscopic studies indicated the polymorphic pair to be monotropic. Solubility studies suggested the relative stability of the two forms to be similar. The infrared (IR) and Raman spectra of the two crystal forms were significantly different, and their complementary nature was shown from the differences in peak intensities. Solid-state ^{13}C-NMR data of the polymorphs showed only minor differences between the two forms. When viewed on the molecular level through the use of vibrational and NMR spectroscopies, the conformation of the molecule in the two polymorphs appears to be roughly equivalent. The magnitude of the spectral differences of the two polymorphs is, however, consistent with those that can be expected for two crystal forms that have resulted from different modes of packing, as caused by the solvent environment.

**Keywords:** *Polymorphs; infrared; Raman; solid-state NMR; crystal packing.*

## Introduction

DuP 747 (Fig. 1) is a selective kappa agonist analgesic that produces potent antinociceptive responses in mice, rats and dogs [1], and was found to exist in at least two polymorphic forms. The current work is aimed at characterizing the polymorphs based on thermal and solubility data and analysing their solid-state characteristics by nuclear magnetic resonance (NMR), IR and Raman spectroscopy.

Infrared and Raman spectroscopy have been widely used to elucidate molecular structures, crystallinity, and polymorphism. The low

frequency Raman modes are particularly useful in distinguishing different molecular packings in crystals [2]. Solid-state ^{13}C-NMR spectroscopy is also used in the characterization of pharmaceutical compounds [3]. [13]C spectra acquired using a combination of cross polarization (CP) [4] for sensitivity enhancement with magic-angle spinning (MAS) [5] and high-power proton decoupling for resolution enhancement have been shown to provide relevant structural and dynamic information [6]. This was demonstrated in a recent report by Raghavan *et al.* [7], which detailed the use of spectroscopic methods, including ^{13}C-CP/MAS NMR, to analyse solid-state characteristics of Losartan polymorphs in relation to their crystal packing. Significant differences in the chemical shift and peak splitting characteristics were observed for the polymorphs, and experiments sensitive to molecular dynamics revealed differences in molecular motion of functional groups at room temperature [7]. As with the other spectroscopic methods used in this study, much of the power of solid-state NMR spectroscopy in the characterization of pharmaceuticals comes from the sampling flexibility that it offers. In the absence of interference due to excipients, drugs may be
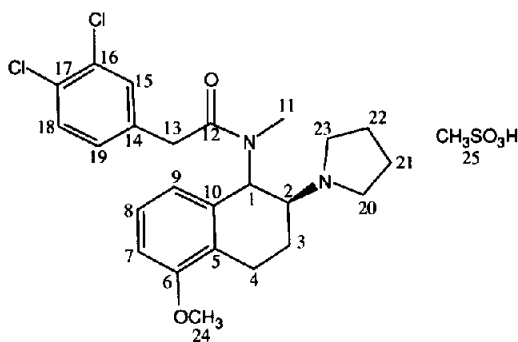
**Figure 1**
DuP 747.

*Author to whom correspondence should be addressed.

studied in their appropriate dosage forms so that the information obtained is pharmaceutically relevant and free of any sample-preparation effects [8].

## Materials and Methods

DuP 747 (racemic *trans*-3,4-dicholoro-N-methyl-N[1,2,3,4-tetrahydro-5-methoxy-2-(pyrrolidin-1-yl)]naphth-1-ylbenzeneacetamide) polymorphs were prepared by the Chemical Processing Division of The DuPont Merck Pharmaceutical Company. Forms I and II were obtained by recrystallizing from 1-propanol and methanol, respectively. The thermal properties of the polymorphs were characterized on a differential scanning calorimeter (Model 910, DuPont Instruments) and a thermogravimetric analyser (Model 951, DuPont Instruments) connected to a data analyser (Thermal analyst 2000, TA Instruments). The thermomicroscopic studies were performed on a polarized light microscope (Leitz Orthoplan-Pol) equipped with a hotstage (Model FP82, Mettler).

The X-ray powder diffraction (XRPD) patterns were recorded using an automated X-ray diffractometer (Phillips APD 3720) with copper tube K alpha radiation.

The solubilities of the two polymorphs were determined in ethyl acetate. Excess powder samples were placed in screw-capped vials containing the solvent and agitated in a thermostated shaking water bath maintained at 25°C. Preliminary studies indicated that no perceptible change in the solubility value occurred after 48 h. After 48 h, the slurry was filtered through a membrane filter (Acrodisc 13 CR PTFE, 0.45 μm, Gelman), with the first portion discarded to ensure saturation of the filter. A known volume of the filtrate was evaporated to dryness (Turbovap LV evaporator, Zymark), reconstituted in a mixture of methanol and water (1:1, v/v) and analysed by HPLC. The solids remaining after the solubility study were analysed by DSC and XRPD.

Liquid chromatography was performed on a system consisting of a pump programmed by a system controller (Model 600E), an auto-injector (Model 712 Wisp), a tunable UV–vis spectrophotometric detector (Model 486) operated at 280 nm, and a column oven programmed by a temperature control module and operated at 45°C, all from Waters (USA). All separations were performed on a Zorbax Rx

$C_8$ column (4.6 mm × 250 mm) using a mixture of methanol and aqueous phase containing octanesulphonic acid sodium salt (5 mM), glacial acetic acid (0.1%) and triethylamine (0.1%) (60:40, v/v) as mobile phase at a flow rate of 2 ml min$^{-1}$. The chromatographic data was acquired and analysed on a VG multichrom system.

Fourier Transform Infrared (FTIR) spectra of the two polymorphs were acquired on an Analect AQS-20 spectrometer equipped with a nitrogen-cooled MCT detector. The samples were mixed with potassium bromide and the spectra were recorded at 4-cm$^{-1}$ resolution using a diffuse reflectance accessory.

Raman spectra were recorded on a Spex 1877 triplemate spectrometer equipped with a photomultiplier tube and optical multichannel detectors. The samples placed in quartz capillary tubes were excited by a 514.5 nm beam from a Coherent Innova-70 argon ion laser. The laser power at the samples was adjusted to about 180 mW and the spectral resolution was about 4 cm$^{-1}$.

Solid-state $^{13}$C nuclear magnetic resonance spectra were acquired at 90.5 and 31.5 MHz using the CP/MAS technique on a Chemagnetics CMX NMR spectrometer equipped with two magnets. A 200 mg mass of each polymorph was used in the acquisition of their respective spectra. All measurements were made at ambient temperature. Chemical shifts are reported on the tetramethylsilane (TMS) scale using hexamethylbenzene as a secondary reference. Solid-state resonance assignments were made using the interrupted decoupling pulse sequence in combination with solution-state $^{13}$C experiments performed on a Varian VXR-400 high-resolution NMR spectrometer.

## Results and Discussion

Recrystallization of DuP 747 from 1-propanol and methanol yields Forms I and II, respectively. The DSC thermograms of Form I (Fig. 2A) and Form II (Fig. 2B) show sharp endotherms at 210.6 and 218.3°C, respectively, at a heating rate of 10°C min$^{-1}$. TGA of Forms I and II did not indicate a weight loss. XRPD patterns (Fig. 3(A) and (B); Table 1) indicate that the two forms have different crystal structures. Heating Form I to 215°C at 10°C min$^{-1}$, cooling to 30°C, and reheating at 10°C min$^{-1}$ resulted in an exotherm at 175°C followed by an endotherm at 218.3°C, indicat-
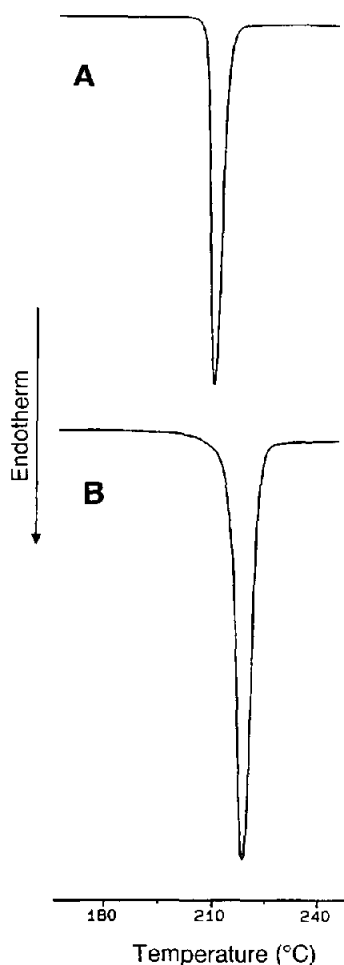
**Figure 2**
DSC thermograms of DuP 747 (A) Form I and (B) Form II. The heating rate was 10°C min⁻¹.

ing a conversion to Form II. Thermomicroscopy of Form I revealed the following events: melting was observed at about 206°C; on cooling the melt, crystallization was observed at approximately 180°C; on reheating, the newly formed crystals melted at 214°C indicating a conversion to Form II. Cooling the melt again resulted in crystallization at approximately 180°C; on reheating, the crystals melted at 214°C, indicating that the event (conversion of Form I to Form II) was not reversible. A solid-state conversion of Form I to Form II was not observed. From these facts it was concluded that the two forms were monotropic. Additional support for the conclusion was given by the 'heat of fusion rule' and the 'heat of transition rule' formulated by Burger and Ramberger [9]. The heat of fusion rule states that 'if the higher melting form has the lower heat of fusion, the two forms are usually enantiotropic; otherwise they are monotropic'. The polymorphic form with the higher melting point (designated Form II) had a higher enthalpy of fusion value ($84.0$ J g⁻¹) than the polymorphic form with the lower melting point (designated Form I; $69.4$ J g⁻¹). The heat of transition rule states that 'if an exothermal transition is observed at some temperature, it may be assumed that there is no transition point below it, i.e. the two forms are related monotropically or the transition temperature is higher'. According to this rule, Form I has no transition point (solid-state conversion) below
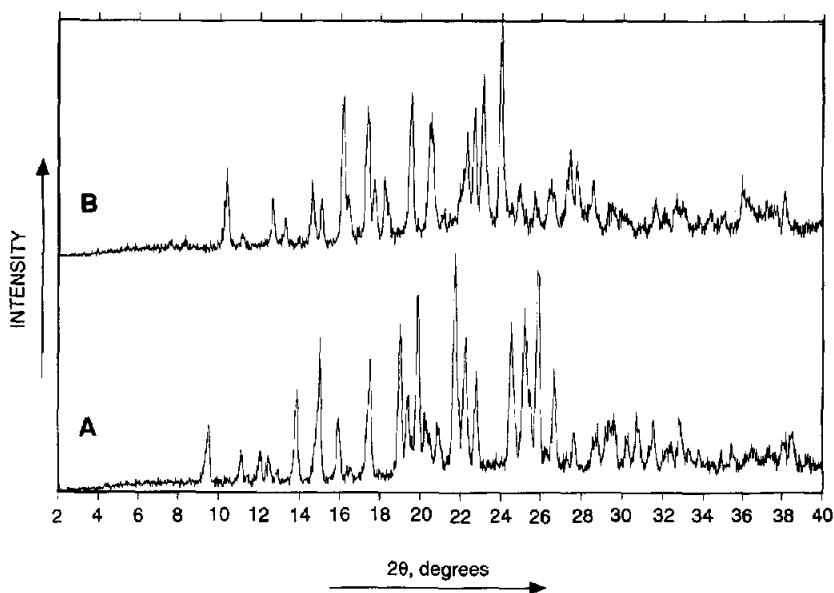


**Figure 3**
X-ray powder diffraction patterns of DuP 747 polymorphs: (A) Form I and (B) Form II.

**Table 1**
Powder X-ray diffraction data of DuP 747 polymorphs

| Form I | | | | Form II | | |
| --- | --- | --- | --- | --- | --- | --- |
| Scattering angle (°2θ) | d-spacing (Å) | Relative intensity (%) | | Scattering angle (°2θ) | d-spacing (Å) | Relative intensity (%) |
| 9.500 | 9.3099 | 28 | | 8.253 | 10.7143 | 3 |
| 11.100 | 7.9713 | 12 | | 10.380 | 8.5225 | 33 |
| 12.043 | 7.3495 | 14 | | 11.108 | 7.9659 | 6 |
| 12.463 | 7.1027 | 13 | | 12.623 | 7.0130 | 23 |
| 12.895 | 6.8654 | 6 | | 13.257 | 6.6785 | 12 |
| 13.875 | 6.3826 | 42 | | 14.592 | 6.0704 | 28 |
| 15.028 | 5.8956 | 65 | | 15.085 | 5.8733 | 22 |
| 15.990 | 5.5429 | 24 | | 16.175 | 5.4799 | 67 |
| 17.515 | 5.0635 | 54 | | 16.445 | 5.3905 | 20 |
| 18.982 | 4.6753 | 73 | | 17.405 | 5.0953 | 60 |
| 19.352 | 4.5867 | 40 | | 17.702 | 5.0103 | 28 |
| 19.885 | 4.4651 | 89 | | 18.190 | 4.8771 | 31 |
| 20.242 | 4.3870 | 28 | | 19.562 | 4.5379 | 67 |
| 20.887 | 4.2530 | 24 | | 20.510 | 4.3304 | 56 |
| 21.725 | 4.0909 | 98 | | 22.322 | 3.9827 | 49 |
| 22.260 | 3.9938 | 63 | | 22.697 | 3.9178 | 56 |
| 22.790 | 3.9021 | 49 | | 23.097 | 3.8505 | 71 |
| 24.535 | 3.6284 | 70 | | 23.985 | 3.7103 | 100 |
| 25.177 | 3.5372 | 74 | | 24.942 | 3.5700 | 24 |
| 25.887 | 3.4418 | 100 | | 25.682 | 3.4688 | 20 |
| 26.660 | 3.3438 | 46 | | 26.390 | 3.3774 | 23 |
| 27.612 | 3.2306 | 20 | | 27.415 | 3.2534 | 37 |
| 28.770 | 3.1032 | 19 | | 27.752 | 3.2146 | 34 |
| 29.445 | 3.0538 | 22 | | 28.550 | 3.1266 | 26 |
| 29.597 | 3.0183 | 24 | | 29.370 | 3.0411 | 15 |
| 30.212 | 2.9582 | 16 | | 30.167 | 2.9625 | 10 |
| 30.685 | 2.9137 | 28 | | 31.622 | 2.8295 | 18 |
| 31.525 | 2.8380 | 27 | | 32.592 | 2.7474 | 16 |
| 32.307 | 2.7710 | 12 | | 32.850 | 2.7265 | 12 |
| 32.853 | 2.7263 | 24 | | 34.330 | 2.6122 | 11 |
| 34.870 | 2.5730 | 6 | | 34.998 | 2.5639 | 10 |
| 35.445 | 2.5326 | 10 | | 35.963 | 2.4973 | 22 |
| 36.395 | 2.4686 | 8 | | 38.095 | 2.3623 | 19 |
| 38.022 | 2.3666 | 12 | | 40.132 | 2.2469 | 10 |
| 38.518 | 2.3373 | 16 | | | | |
| 40.180 | 2.2444 | 6 | | | | |

175°C. Above this temperature, the only event observed was the melting of Form II.

The free energy difference ($\Delta F_{I,II}$) between the two polymorphs is an indication of their relative stability, and can be obtained by means of solubility measurements according to the formula

$$\Delta F_{I,II} = RT \ln \frac{\text{solubility of Form I}}{\text{solubility of Form II}}, \quad (1)$$

where $T$ is the temperature (K) at which the solubilities were determined and $R$ is the gas constant [10]. The solubilities of Form I and II in ethyl acetate at 25°C were 719 ± 2.63 and 618 ± 3.96 μg ml$^{-1}$ (mean ± SD; $n = 3$), respectively. The solubility ratio, i.e. (solubility of Form I)/(solubility of Form II) in ethyl acetate was found to be 1.16, and the free energy difference between the polymorphs was

89.6 cal mol$^{-1}$. The small difference in free energy of the two polymorphic forms suggests a small difference in their relative stability. DSC and XRPD patterns were obtained on the solids remaining after the solubility study had been completed; no polymorphic conversion had taken place in either case during the solubility study.

Infrared and Raman spectra of the polymorphs are shown in Figs 4–7; while no attempt was made to assign all the peaks in the spectra, the regions where significant differences were observed for the two polymorphs have been assigned based on published literature on related molecules [11]. Infrared and Raman spectra for the two polymorphs revealed several significantly different spectral features. Especially noticeable was the absence or attenuation of certain vibrational modes in the Raman spectra that were very pronounced
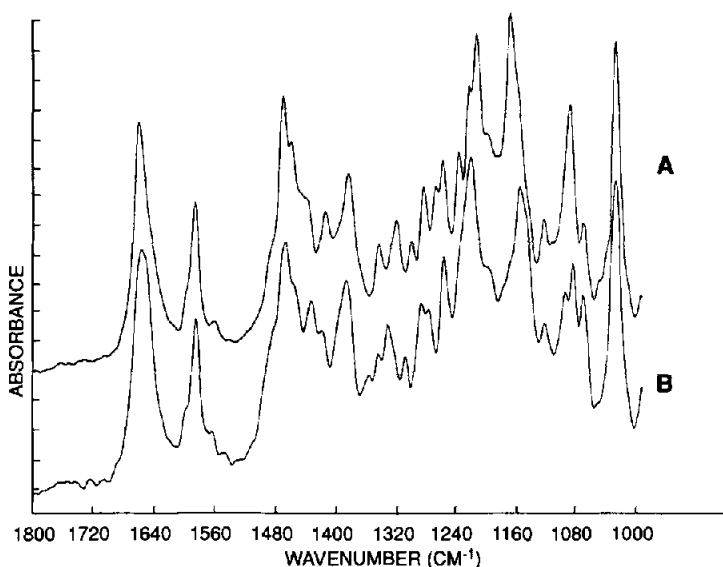
**Figure 4**
FTIR Spectra of DuP 747 polymorphs from 1800 cm$^{-1}$ to 1000 cm$^{-1}$: (A) Form I and (B) Form II.
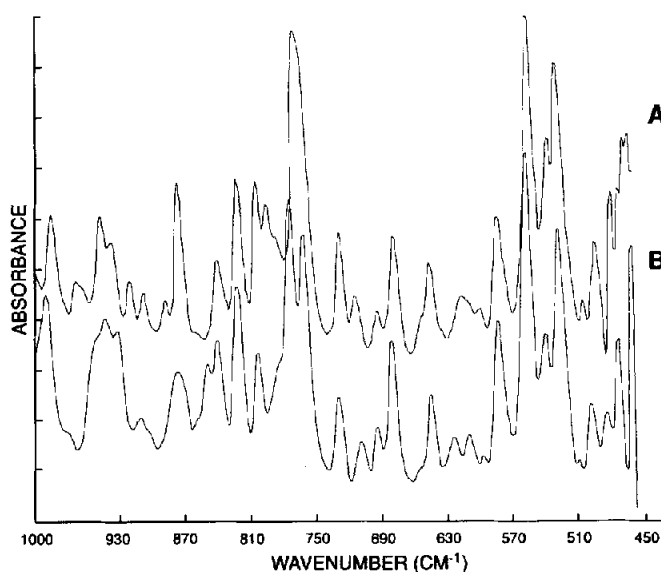


**Figure 5**
FTIR Spectra of DuP 747 polymorphs from 1000 cm$^{-1}$ to 450 cm$^{-1}$: (A) Form I and (B) Form II.

in the IR spectra, and vice versa. This is because the mechanism of interaction of electromagnetic radiation with matter is different in the two spectroscopic techniques. The IR absorption is caused by changes in dipole moment associated with molecular vibration, while the Raman scattering arises due to changes in the polarizability of the molecule associated with a vibration. Usually, asymmetric modes and those associated with polar functional groups are stronger in IR and weaker in Raman, and the symmetric modes and those associated with non-polar functional groups are stronger in Raman and weaker in IR. For instance, a strong band around 1470 cm$^{-1}$ associated with the $CH_3$ asymmetric bending vibration was observed in the IR spectra of both polymorphs, whereas the Raman spectra showed a weak shoulder around 1470 cm$^{-1}$ in Form I and a complete absence of this mode in Form II. Although the $CH_3$ asymmetric bending modes are relatively weaker in Raman, a complete absence of this mode in Form II indicates that the methyl
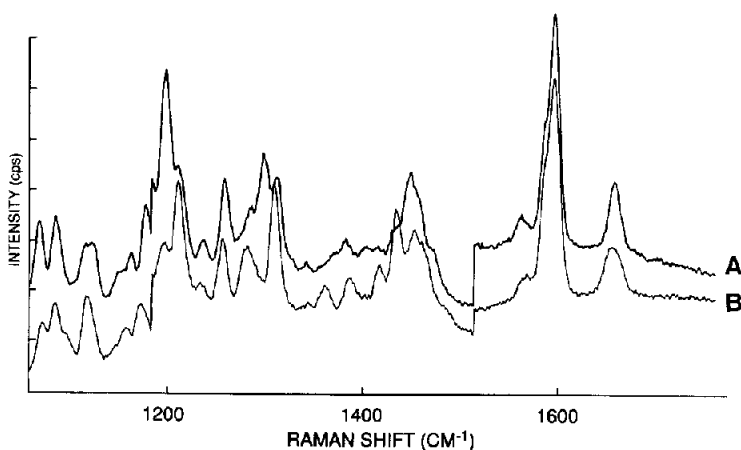
**Figure 6**
Raman spectra of DuP 747 polymorphs from 1100 to 1800 cm$^{-1}$: (A) Form I and (B) Form II.
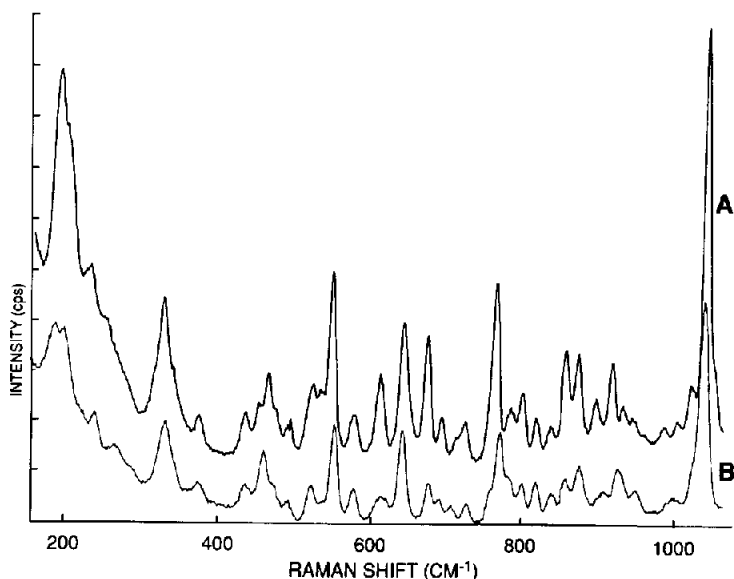


**Figure 7**
Raman spectra of DuP 747 polymorphs from 180 to 1000 cm$^{-1}$: (A) Form I and (B) Form II.

groups are positioned differently in this polymorph. The spectral region in Raman associated with $CH_2$ angle bending modes (1440–1460 cm$^{-1}$) shows distinct differences between the two polymorphs. In Form I a broad band around 1451 cm$^{-1}$ and a weak shoulder around 1436 cm$^{-1}$ were observed, whereas in Form II two sharper bands around 1454 and 1436 cm$^{-1}$ were observed with a reversed intensity pattern. Infrared spectra of both polymorphs showed similar features in this region. Two Raman bands associated with $CH_3$ symmetric bending vibrations were observed at 1388 and 1362 cm$^{-1}$ in Form II, and at 1383 and 1375 cm$^{-1}$ in Form I. In contrast, IR spectra show only one band at 1390 cm$^{-1}$ in Form II, and at

1387 cm$^{-1}$ in Form I. Raman spectra also show different splitting patterns in the $CH_2$ twist vibrations of the two polymorphs; two bands at 1162 and 1176 cm$^{-1}$ in Form II and three bands at 1156, 1166 and 1182 cm$^{-1}$ in Form I were observed. No such splitting pattern was observed in the IR spectra, which show one mode at 1162 cm$^{-1}$ for Form II and one at 1173 cm$^{-1}$ for Form I.

The modes associated with the rings also show differences in the two polymorphs. Strong peaks observed in the IR spectra at 1226 cm$^{-1}$ in Form II, and at 1228, 1218 and 1242 cm$^{-1}$ in Form I have been assigned to aryl C—O—C stretching vibrations. This mode observed around 1239 cm$^{-1}$ in Raman for both

polymorphs is rather weak. In contrast, the modes associated with aryl-alkyl C—C stretching vibrations are strong in Raman and show reversed intensity pattern (1202/1214 cm$^{-1}$ in Form I and 1199/1214 cm$^{-1}$ in Form II) in the two polymorphs. In IR a very weak aryl-alkyl C—C stretching mode is observed at 1202 cm$^{-1}$ for both polymorphs. In the spectral region of 920–1040 cm$^{-1}$ associated with ring in-plane stretching vibrations mixed with C—H in-plane bending vibrations, Raman seems to be more sensitive to the differences between the two polymorphs. This is shown by a significant difference in the splitting pattern of the modes. Raman bands for Form I in this region were observed at 1035, 1018, 1000, 983, 942 and 928 cm$^{-1}$, while the corresponding modes in Form II appeared at 1032, 993, 947 and 923 cm$^{-1}$. The IR modes in this region were observed at 962, 941 and 932 cm$^{-1}$ in Form I and at 945, 937 and 926 cm$^{-1}$ in Form II. The IR modes in the 920–700 cm$^{-1}$ region, primarily associated with C—H out of plane bending modes, showed significant differences in spectral resolution and intensity for the two polymorphs, suggesting different orientations of the aromatic rings. However, Raman modes in this spectral region were not so sensitive to differences between the two polymorphs.

Raman provides a wealth of information in the low frequency region not observed in the mid IR. The Raman modes in this region are very sensitive to structural changes in the solid state such as crystal packing, size and shape of the unit cell, and intermolecular interactions. In this region, Form I showed Raman bands at 549, 536, 525, 467 and 455 cm$^{-1}$, while Form II had three modes at 553, 525 and 462 cm$^{-1}$. These modes are associated with out-of-plane ring deformations. Further, in the low frequency region associated with lattice vibrational modes, the two polymorphs showed differences in their splitting pattern. Form I had three modes at 192, 233 and 254 cm$^{-1}$, whereas Form II had five modes at 188, 200, 242, 270 and 291 cm$^{-1}$.

The solid-state $^{13}$C-CP/MAS NMR spectra of the two polymorphs of DuP 747 are shown in Fig. 8. The overall appearance of the $^{13}$C-NMR spectra of the two polymorphs is quite similar. Table 2 lists the chemical shifts for the two solid polymorphs and compares them to the corresponding $^{13}$C solution-state values. The data reflect the close correspondence of

observed chemical shifts. However, there are small but real differences between the chemical shift positions of the carbon atoms of the two polymorphs. The carbon resonance corresponding to C10 shows the largest shift difference (almost 4 ppm), while most other sites have chemical shifts that differ by less than about 2 ppm for the two solid polymorphs. There are no signal multiplicity differences between the two polymorphs at any of the resonance positions observed even though the spectral traces do not appear to be rigorously superimposable. The resonance at 21.9 ppm in Form I, for example, appears to be split (21.1 and 23.3 ppm) in Form II. Instead of being related to structural differences in the unit cells of the two polymorphs, the resonances for C3 and C4 are unresolved and appear as one peak at 21.9 ppm in Form I. Other spectral differences seen in Fig. 8 for the two polymorphs are similarly rationalized.

One interesting difference between the $^{13}$C solid-state NMR results for the two polymorphs of DuP 747 had to do with their response to the interrupted decoupling, or dipolar dephasing experiment. This technique is closely related to the normal CP experiment except that the $^1$H decoupler is turned off for a short period of time (40 μs) before final $^{13}$C signal acquisition under high-power proton decoupling. This brief 'switching on' of the proton dipolar interaction causes a loss of spectral resolution at carbon sites with tightly coupled protons. Practically, resonances for methylene and methine carbons are not observed in the interrupted decoupling experiment, and the spectrum contains only signals attributable to nonprotonated and methyl carbons. The latter generally survive the interrupted decoupling due to motional modulation of the $^1$H–$^{13}$C dipolar interaction.

In Form I, resonances respond to the interrupted decoupling experiment in ways that are expected, given their chemical shifts and the included solution-state results. The same is not true in Form II as the $^{13}$C signal assigned to methylene carbon C13 (near 40 ppm) survives 40 μs of interrupted decoupling. This indicates that, at ambient temperature, there is some motional modulation of the carbon–hydrogen dipolar interaction that is either rapid and/or isotropic. Such motion could perhaps be a bending or twisting of the 'elbow' at C13 between the carbonyl group and the dichlorobenzene ring. This added degree of molecular
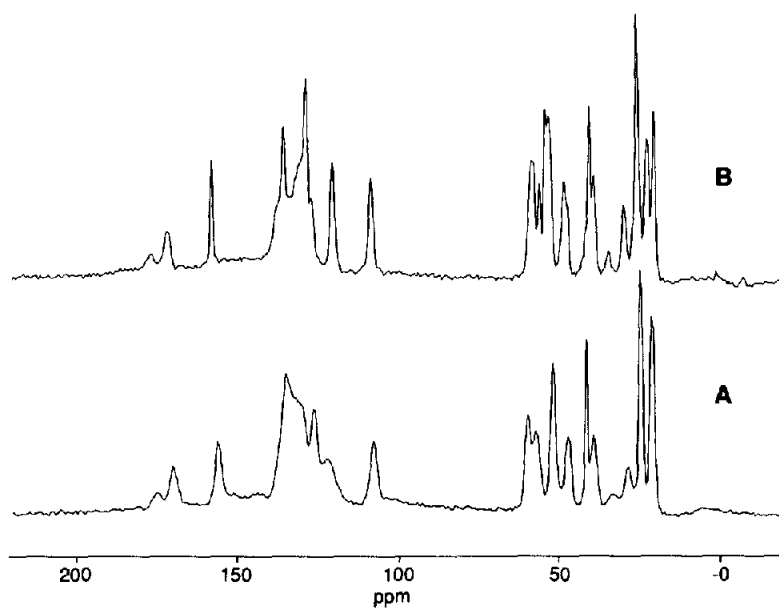
**Figure 8**
Solid-state $^{13}$C-CP/MAS NMR spectra of DuP 747 polymorphs: (A) Form I and (B) Form II.

**Table 2**
Solution $^{13}$C-NMR chemical shifts for DuP 747 in deuterated chloroform
and $^{13}$C-CP/MAS solid-state NMR chemical shifts for Form I and Form II

| | | $^{13}$C chemical shifts [ppm] | |
| | | Solid state | |
| Carbon number | Solution [CDCl$_3$] | Form I | Form II |
|---|---|---|---|
| 1 | 54.5 | 53.9 | 54.8 |
| 2 | 59.7 | 60.3 | 59.2 |
| 3 | 20.6 | 21.9 | 21.1 |
| 4 | 22.1 | * | 23.3 |
| 5 | 125.1 | 126.3 | 126.9 |
| 6 | 156.9 | 156.1 | 158.1 |
| 7 | 108.8 | 108.2 | 109.0 |
| 8 | 128.0 | * | 129.2 |
| 9 | 118.7 | 122.1 | 120.6 |
| 10 | 133.2 | 134.1 | 129.2 |
| 11 | 31.3 | 30.7 | 32.0 |
| 12 | 174.1 | 172.0 | 174.0 |
| 13 | 39.9 | 39.6 | 39.7 |
| 14 | 135.7 | 137.0 | 139.0 |
| 15 | 131.9 | 130.8 | 131.0 |
| 16 | 132.1 | 134.1 | 136.1 |
| 17 | 130.7 | 134.1 | 136.1 |
| 18 | 130.2 | 130.8 | 131.0 |
| 19 | 129.6 | 130.8 | 131.0 |
| 20 | 52.2 | 52.3 | * |
| 21 | 24.2 | 25.4 | 26.7 |
| 22 | 23.9 | 25.4 | 26.7 |
| 23 | 48.4 | 47.7 | 48.0 |
| 24 | 55.4 | 57.9 | 56.5 |
| 25 | 39.3 | 42.1 | 41.3 |

All chemical shifts are relative to tetramethylsilane and numbered carbon
atoms refer to the structure in Fig. 1. *Not resolved.

motion seems consistent with a loosely packed crystal structure for Form II.

In summary, DuP 747 was found to exist in at least two polymorphic forms. XRPD was used to confirm this. DSC was used along with thermomicroscopy to establish that the two forms were monotropically related. Solubility studies indicated that the relative stability for the two polymorphs was similar. FTIR and Raman spectra of the two forms revealed significant differences concurring with the conclusion drawn from the XRPD data that the crystal packing in the two polymorphs were different. The solid-state $^{13}$C-NMR of the two polymorphs were very similar with small but real differences between the chemical shift positions of the carbon atoms of the two polymorphs. These differences are as large as can be expected for two crystalline polymorphs that have resulted from different modes of packing, as caused by the solvent environment. The nature of the polymorphism reported here does not appear to be associated with variations in molecular conformation. When viewed on the molecular level through the use of vibrational and NMR spectroscopies, the conformation of the molecule in the two polymorphs appears to be roughly equivalent. However, the details of the crystal packing and molecular conformation of the polymorphs await crystallographic information.

## References

[1] W.K. Schmidt, P. Rajagopalan, L. Cook, M.E. Marynowski, S.W. Tam, L.C. Johnson, G.F. Steinfels, R.M. Scribner, P. Pennev, P.L. Mattei and A.L. Johnson, American Chemical Society (ACS) 200th meeting, Washington D.C., Abstracts, p.59-MEDI (1990).

[2] J.C. Decius and R.M. Hexter, Molecular Vibrations in Crystals. McGraw Hill, New York (1977).

[3] H.Y. Aboul-Enein, Spectroscopy 5, 32–40 (1990).

[4] A. Pines, M.G. Gibby and J.S. Waugh, J. Chem. Phys. 59, 569–590 (1973).

[5] E.R. Andrew, A. Bradbury and R.G. Eades, Nature 183, 1802–1803 (1959).

[6] S.R. Byrn, B. Tobias, D. Kessler, J. Frye, P. Sutton, P. Saindon and J. Kozlowski, Trans. Am. Crystallogr. Assoc. 24, 41–54 (1989).

[7] K. Raghavan, A. Dwivedi, G. Campbell Jr, E. Johnston, D. Levorse, J. McCauley and M. Hussain, Pharm. Res. 10, 900–904 (1993).

[8] P.J. Saindon, N.S. Cauchon, P.A. Sutton, C.-J. Chang, G.E. Peck and S.R. Byrn, Pharm. Res. 10, 197–203 (1993).

[9] A. Burger and R. Ramberger, Mikrochim. Acta 11, 259–271 (1979).

[10] W.I. Higuchi, P.K. Lau, T. Higuchi and J.W. Shell, J. Pharm. Sci. 52, 150–153 (1963).

[11] D. Lin-Vein, N.B. Colthup, W.G. Fateley and J.G. Grasselli, The Handbook of Infrared and Raman Characteristic Frequencies of Organic Molecules. Academic Press, New York (1991).